

Thermal effects in InP/(Ga,In)P quantum-dot single-photon emitters

A. K. Nowak,¹ E. Gallardo,¹ D. Sarkar,^{1,2} H. P. van der Meulen,¹ J. M. Calleja,¹ J. M. Ripalda,³ L. González,³ and Y. González³

¹*Departamento de Física de Materiales, Universidad Autónoma de Madrid, E-28049 Madrid, Spain*

²*Department of Physics and Astronomy, University of Sheffield, Sheffield S3 7RH, United Kingdom*

³*Instituto de Microelectrónica de Madrid, Centro Nacional de Microelectrónica, Consejo Superior de Investigaciones Científicas, Isaac Newton 8, PTM Tres Cantos, E-28760 Madrid, Spain*

(Received 14 July 2009; revised manuscript received 29 September 2009; published 14 October 2009)

We present second-order photon correlation measurements on single InP/(Ga,In)P quantum dots as a function of temperature. Low background emission allows to obtain antibunching minima $g^{(2)}(0)$ below 0.25 up to 45 K. The antibunching time τ_R increases or decreases with temperature depending on the quantum-dot size. The two trends result from a competition between hole thermal excitation and dark-to-bright exciton transitions. The former prevails in smaller dots showing increasing τ_R with temperature, while the latter dominates in larger quantum dots showing decreasing τ_R with temperature.

DOI: [10.1103/PhysRevB.80.161305](https://doi.org/10.1103/PhysRevB.80.161305)

PACS number(s): 78.67.Hc, 78.55.Cr, 42.50.Ar

Semiconductor quantum dots (QDs) are among the most promising single-photon emitters (SPEs) for quantum information applications due to their versatility, scalability, and ease to handle as compared to atom or ion-based SPEs.^{1–4} However, the use of semiconductor QDs as true “on demand” SPEs is conditioned by the presence of “background photons” (photons emitted outside the QD but at the QD energy) and decoherence.⁵ One important source of decoherence in QDs is the random transition between bright exciton (BX) and dark exciton (DX) states (exciton states with total angular momentum 1 and 2, respectively).⁶ Exciton energy splittings, as the dark-bright exciton splitting E_{DB} and the fine-structure splitting Δ_{FS} , which are large in QDs as compared to higher dimensional systems due to the increased electron-hole Coulomb interaction, are strongly sensitive to the QD size and shape.^{7–9} InP QDs have received special attention for their potential use as SPEs in the visible range.^{10–16} Photon correlation measurements for both continuous^{9,11} and pulsed excitation^{11,13,15} as well as under electrical injection¹⁴ show clear antibunching dips in the second-order photon correlation function $g^{(2)}(\tau)$ at zero delay ($\tau=0$). The standard form of the correlation function is

$$g^{(2)}(\tau) = 1 - \beta \exp(-|\tau|/\tau_R), \quad (1)$$

where τ_R is the characteristic (minimum) time needed for the emission of a second photon after the first one has been emitted by the QD and β is generally determined by background photons. A value $\beta=1$ indicates perfect SPE. The low values of $g^{(2)}(0)$ found in InP QDs (between 0.1 and 0.2) (Refs. 10–15) is indicative of efficient single-photon emission. High-temperature operation of a SPE is beneficial for practical uses. Antibunching dips up to 200 K have been reported for GaN (Ref. 17) and CdSe (Ref. 18) QDs and up to 90 K in InGaAs/AlGaAs QDs.¹⁹ In InP QDs an upper limit of 80 K has been reached using Al containing barriers.¹³ Upon raising temperature the $g^{(2)}(0)$ value progressively increases due to the increasing background luminescence. Temperature also influences the antibunching width. Indeed τ_R depends on several factors, as the pumping rate, the exciton lifetime²⁰ and the carrier relaxation time, some of them

being temperature dependent. An increase in τ_R with temperature has been reported in InGaAs/AlGaAs QDs.¹⁹

In this Rapid Communication we present photon correlation measurements on small InP/GaInP QDs to study the effect of temperature on $g^{(2)}(0)$ and τ_R . Single QDs are selected that emit at high energies, well outside the ensemble photoluminescence (PL) emission, to minimize the interdot contribution to the background emission. We obtain $g^{(2)}(0)$ values below 0.25 up to 45 K, as a result of the low background. Increasing temperature produces either an increase or a decrease in τ_R depending on the QD size. The size is inferred from the relative values of the biexciton binding energy E_b^{XX} and the fine-structure splitting Δ_{FS} .⁸ We propose a competition between the dark-to-bright exciton transition (governed by E_{DB}) and thermal excitation of holes (governed by an effective interhole energy spacing E_h) to explain the different behavior of τ_R . Thermal hole excitation is dominant for smaller QDs in which τ_R increases with temperature,¹⁹ while dark-to-bright exciton transitions are favored in larger QDs, showing decreasing τ_R .

The QD samples have been grown by molecular-beam epitaxy on GaAs (001) substrates. The growth sequence was 100 nm GaInP, 2 monolayers (ML) GaAs, and 2.2 ML InP, repeated twice. The critical thickness for QD nucleation at 470 °C was 2 ML of InP at a growth rate 0.05 ML/s. The second uncapped layer of QDs was used for atomic force microscopy characterization. The QD average diameter and height before capping are 35 and 6 nm, respectively. However, the single QD selected for this work are far in the high energy tail of the ensemble PL so that their height is much less than 6 nm. From their PL energies we estimate it to be between 1 and 2 nm.¹⁵ PL spectra of QDs were taken through a 100× microscope objective (1.5 μ m spot size) under non-resonant excitation using a He-Ne laser and a charge coupled device detector located at one of the exits of a 0.75 cm focal length spectrometer. The photon correlation measurements were done with a Hanbury-Brown and Twiss (HBT) interferometer located at the second exit of the spectrometer. Two avalanche photodiodes with 65% efficiency at the QD emission energy (1.86 eV) were used for coincidence detection.

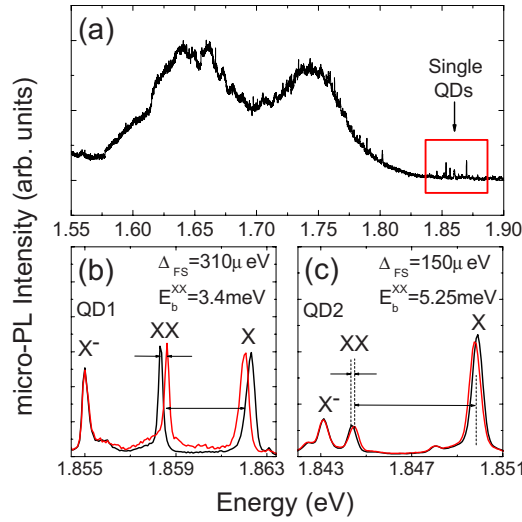


FIG. 1. (Color online) (a) PL spectrum of the InP/GaInP QD ensemble. (b) and (c) PL spectra of single quantum dots: QD1 and QD2, respectively. The black and red lines represent polarization parallel to the [110] and [1-10] crystallographic directions, respectively. The chosen quantum dots exhibit large differences in the binding energy E_b^{XX} and the fine-structure splitting Δ_{FS} indicating different QD size and/or shape.

Their response time ($\tau_i = 0.5$ ns) was measured with 2 ps pulses of a Ti-sapphire laser. Count rates at the detectors were up to 10^4 counts/s. The ensemble PL spectrum of the QDs is presented in Fig. 1(a). Single QDs were selected in the 1.84–1.87 eV emission range, well above the average emission energy. This ensures small QD size allows spectral isolation of single QD emission lines and prevents charge transfer from neighboring QDs. The micro-PL spectra of two different quantum dots are shown in Figs. 1(b) and 1(c) for relatively high excitation power. Three lines (exciton X, biexciton XX, and negatively charged exciton X^-) are identified by their intensity dependence on excitation power (not shown) and linear polarization. Black and red traces correspond to linear polarization parallel to the [110] and [1-10] crystallographic directions, respectively. Significant differences in the biexciton binding energy (E_b^{XX}) and the fine-structure splitting are observed between QD1 and QD2. Both the smaller value of E_b^{XX} and the higher value of Δ_{FS} indicate stronger electron-hole exchange energy⁸ in QD1. As exchange energy depends on the electron-hole wave-function overlap, we infer that QD1 is significantly smaller in height than QD2.

The second-order photon autocorrelation function of the exciton was measured for both quantum dots in the temperature range between 5 and 45 K. The result for QD2 at 5 K is shown in Fig. 2. Solid and dashed lines are fits to Eq. (1) with $g_{CONV}^{(2)}(\tau)$ and without $g^{(2)}(\tau)$ convolution with the instrumental time response function, respectively, which is proportional to $\exp(-|\tau|/\tau_i)$.¹⁴ As the background PL intensity is only 2% of the QD emission, no background correction was done.²¹ The $g^{(2)}(0)$ and τ_R values corrected for the instrumental response time are 0.07 ± 0.05 and 0.63 ± 0.16 ns, respectively. Error bars resulting from fit to Eq. (1) are mainly due to the relatively high noise level in the HBT histogram.

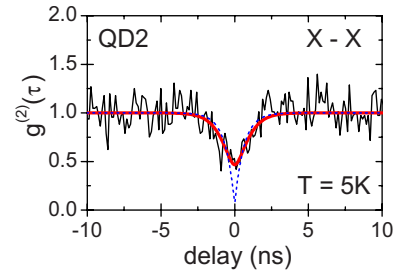


FIG. 2. (Color online) Second-order correlation function of X emission from QD2. The solid and dashed lines are theoretical fits to Eq. (1) with $g_{CONV}^{(2)}(\tau)$ and without $g^{(2)}(\tau)$ convolution with the instrumental time response function, respectively. The strong antibunching minimum at zero time delay implies close to ideal single-photon emission from the QD.

The variations of $g^{(2)}(0)$ and τ_R with temperature constitute the main point of this Rapid Communication. We will discuss them together with the temperature dependence of the PL intensity ratio $I_X/(I_X + I_{XX})$, where I_X and I_{XX} are the exciton and biexciton emission intensities, respectively, to get better insight into the involved mechanisms. The temperature dependence of $I_X/(I_X + I_{XX})$, τ_R and $g_{CONV}^{(2)}(0)$, are shown in Fig. 3 for QD1 [Figs. 3(a), 3(c), and 3(e)] and QD2 [Figs. 3(b), 3(d), and 3(f)], respectively. The data correspond to low excitation intensity so that $I_{XX} \leq 0.15 I_X$. We observe marked differences between QD1 and QD2. The intensity ratio increases steadily with temperature for QD1 while it is almost constant up to 40 K for QD2 and increases at higher

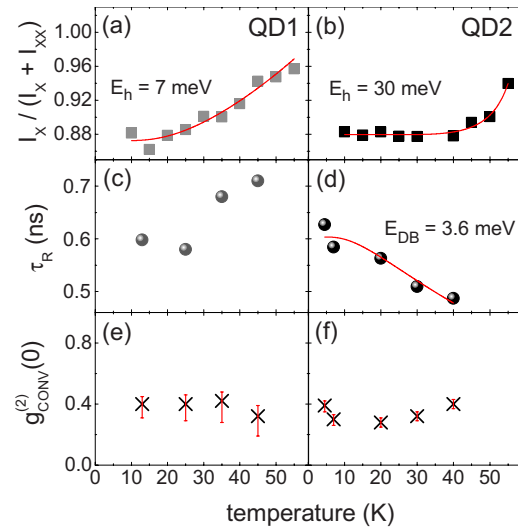


FIG. 3. (Color online) Temperature dependence of quantum-dot properties for QD1 (left) and QD2 (right): (a) and (b) PL intensity ratio $I_X/(I_X + I_{XX})$, where I_X and I_{XX} are the exciton and biexciton intensities, respectively. The solid lines are fits to Eq. (3). (c) and (d) Characteristic antibunching time τ_R . The solid line is the fit to Eq. (4). The differences between QD1 and QD2 observed both in the PL intensity ratio and in τ_R show competition between hole thermal excitation and dark-to-bright exciton transition processes. (e) and (f) Antibunching minima obtained from the experimental data before deconvolution with the instrumental time response function.

temperatures. The antibunching time increases for QD1 and decreases for QD2, as shown in Figs. 3(c) and 3(d).

Among the possible mechanisms influencing τ_R (exciton lifetime, pump rate, etc.)²⁰ and $I_X/(I_X+I_{XX})$, there are at least two temperature dependent ones: dark-to-bright exciton transitions^{22,23} ($D \rightarrow B$) and thermal excitation of holes.¹⁹ The first one is expected to reduce τ_R as $D \rightarrow B$ events produce bright excitons in addition to those formed by direct capture of an electron-hole pair (EHP) with proper angular momenta by the QD. The second mechanism (hole excitation) increases τ_R as it reduces the probability of ground-state exciton formation. We discuss next the effect of both mechanisms on $I_X/(I_X+I_{XX})$ and τ_R .

$D \rightarrow B$ transitions have been claimed as the origin of the $I_X/(I_X+I_{XX})$ increase with temperature, and E_{DB} values between 1.4 and 5 meV have been reported in small InP QDs.¹⁵ Thermal hole excitation will also increase $I_X/(I_X+I_{XX})$. It decreases the emission probability of both X and XX , but while excitation of the only hole present in X just reduces I_X , excitation of one of the two holes present in XX reduces I_{XX} and leaves a new exciton. Thus I_{XX} is expected to decrease faster than I_X upon thermal excitation of holes. Which mechanism dominates will depend on the respective characteristic energies: E_{DB} for $D \rightarrow B$ and E_h for hole excitation. In our case, a data fit with an Arrhenius-type law involving $D \rightarrow B$ processes¹⁵ gives activation energies of the order of tens of meV for QD1 and QD2. These values are inconsistent with any reasonable estimate of E_{DB} in InP QDs.^{15,24} Instead, they are close to the expected values of the excited hole states, so that thermal excitation of holes could account for the observed temperature trend in our case. A rough estimate of E_h can be obtained assuming that I_X and I_{XX} decrease with temperature according to

$$I_X = A - BN,$$

$$I_{XX} = C - DN,$$

$$N = [\exp(E_h/kT) - 1]^{-1}, \quad (2)$$

where N is the Bose-Einstein occupation factor of the phonons responsible for the hole excitation, and A , B , C , and D are temperature independent constants. Then we have

$$\frac{I_X}{I_X + I_{XX}} = \frac{1 - aN}{b - cN}, \quad (3)$$

where $a = B/A$, $c = (B+D)/A$, and $b = 1 + C/A$. The parameter b is fixed by the intensity ratio at low temperature. The fit of our $I_X/(I_X+I_{XX})$ data with Eq. (3) [continuous lines in Figs. 3(a) and 3(b)] gives $E_h = 7$ and $E_h = 30$ meV for QD1 and QD2, respectively. These values are compatible with the heavy-light hole splitting in our QDs, which show a weak hole confinement. Actually the valence-band offset of unstrained InP/InGaP is negative ($\Delta E_v = -45$ meV) (Ref. 25) so that holes are solely confined by strain. In our small QDs only one pair of confined hole states (heavy and light) is expected. For a 1-nm-high QD with rectangular confinement potential and positive valence-band offset of 50 meV, a heavy-light hole splitting of $E_h = 6$ meV is expected. This

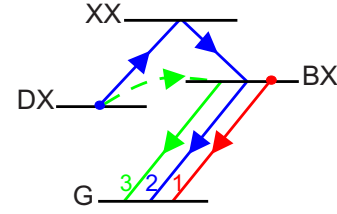


FIG. 4. (Color online) Level scheme including: QD ground state (g), DX, BX, and biexciton (XX). The arrows (1, 2, and 3) represent the photon emission of the bright exciton state after three possible ways of charging.

value increases upon increase of the QD height, i.e., moving from QD1 to QD2.

Going now to τ_R we recall that our measurements are done at low excitation intensities. In these conditions bright excitons recombine before capture of a second EHP to form a biexciton. Biexcitons are thus formed mainly from dark excitons, while bright excitons can result from three different channels (see Fig. 4): (1) capture by the empty QD of an EHP with antiparallel angular momenta directly from the wetting layer (red arrow), (2) emission of a biexciton photon (blue arrows), and (3) a thermally activated $D \rightarrow B$ exciton transition assisted by acoustic phonons.²³ The two first channels are roughly temperature independent. Thus, the antibunching time τ_R can be represented by

$$\frac{1}{\tau_R} = \frac{1}{\tau_A} + \frac{1}{\tau_B},$$

$$\frac{1}{\tau_B} = A[\exp(E_{DB}/kT) - 1]^{-1}, \quad (4)$$

where $1/\tau_A$ is the combined transition probability for channels 1 and 2, while $1/\tau_B$ stands for channel 3. Here we assume a $D \rightarrow B$ transition activated by acoustic phonons with energies close to E_{DB} . The temperature trend of QD2 is properly described by Eq. (4) [solid line in Fig. 3(d)] giving $E_{DB} = 3.6$ meV. E_{DB} values of this magnitude are not surprising in spite of the lower values found in InAs QDs.^{26,27} In fact, values of the order of a few meV have been reported both theoretically²⁴ and experimentally¹⁵ in small InP QDs due to the increased electron-hole exchange interaction. This is also consistent with the high E_{DB} value (2 meV) found in CdSe QDs with a fine-structure splitting (200 μeV) (Ref. 28) comparable to the present ones (150–300 μeV). In the smaller QD1 we expect a larger value of E_{DB} due to the increased electron-hole overlap and a lower E_h due to the increased confining energy. The increasing trend of τ_R with temperature indicates that thermal excitation of holes takes over $D \rightarrow B$ processes ($E_h \leq E_{DB}$) in QD1. Indeed, if the probability of finding a hole in the ground state decreases, the average time needed to “recharge” the QD after emission of a bright exciton photon will increase. As a result E_h dominates at low T and τ_R increases with temperature in QD1. In the larger QD2 it is the other way around. Smaller E_{DB} and larger E_h values lead to $E_h > E_{DB}$. In this case E_{DB} dominates over E_h at low temperature, leading to a τ_R decrease.

As a final remark, we note that the $g_{\text{CONV}}^{(2)}(0)$ values obtained from the raw experimental data reported in this work remain below 0.48 and 0.43 for QD1 and QD2, respectively, as shown in Figs. 3(e) and 3(f) for the whole temperature range. Deconvolution of the experimental data with the instrumental time response function returns average $g^{(2)}(0)$ values below 0.25 for both QDs, without the need of background subtraction. The low $g^{(2)}(0)$ values reported here open good perspectives to use these small InP QDs as efficient SPEs at moderate temperatures.

In summary we present joint PL and photon correlation measurements in small, well isolated InP/InGaP quantum dots that show different trends with increasing temperatures depending on the QD size. In the smaller dot (QD1) the

temperature behavior is governed by the hole excitation energy, leading to an increase of both the intensity ratio $I_X/(I_X+I_{XX})$ and the antibunching time τ_R . In the larger dot (QD2) the low-temperature behavior is fixed by the smaller value of the dark-bright exciton splitting, giving rise to a decreasing τ_R with temperature and an essentially temperature independent intensity ratio.

This work has been supported by research contracts of the Spanish Ministry of Education (Grant No. MAT2008-01555/NAN), Consolider CSD (Grant No. 2006–19), the Community of Madrid (Grant No. CAMS-0505-ESP-0200), and the Spanish Ministry of Science and Innovation (Grant No. Nanoinpho-QD TEC2008-06756-C03-01).

-
- ¹P. Michler, A. Imamoglu, M. D. Mason, P. J. Carson, G. F. Strouse, and S. K. Buratto, *Nature (London)* **406**, 268 (2000).
- ²P. Michler, A. Kiraz, C. Becher, W. V. Shoenfeld, P. M. Petroff, L. Zhang, E. Hu, and A. Imamoglu, *Science* **290**, 2282 (2000).
- ³C. Santori, M. Pelton, G. Solomon, Y. Dale, and Y. Yamamoto, *Phys. Rev. Lett.* **86**, 1502 (2001).
- ⁴V. Zwiller, H. Blom, P. Jonsson, N. Panev, S. Jeppesen, T. Tsegaye, E. Goobar, M.-E. Pistol, L. Samuelson, and G. Björk, *Appl. Phys. Lett.* **78**, 2476 (2001).
- ⁵V. Zwiller, T. Aichele, and O. Benson, *Phys. Rev. B* **69**, 165307 (2004); K. Bando and Y. Masumoto, *J. Lumin.* **128**, 855 (2008).
- ⁶J. D. Cuthbert and D. G. Thomas, *Phys. Rev.* **154**, 763 (1967); P. Palinginis, H. Wang, S. V. Goupalov, D. S. Citrin, M. Dobrowolska, and J. K. Furdyna, *Phys. Rev. B* **70**, 073302 (2004); S. V. Goupalov, R. A. Suris, P. Lavallard, and D. S. Citrin, *IEEE J. Sel. Top. Quantum Electron.* **8**, 1009 (2002).
- ⁷M. Bayer, G. Ortner, O. Stern, A. Kuther, A. A. Gorbunov, A. Forchel, P. Hawrylak, S. Fafard, K. Hinzer, T. L. Reinecke, S. N. Walck, J. P. Reithmaier, F. Klopff, and F. Schäfer, *Phys. Rev. B* **65**, 195315 (2002).
- ⁸G. A. Narvaez, G. Bester, and A. Zunger, *Phys. Rev. B* **72**, 245318 (2005).
- ⁹S. Rodt, A. Schliwa, K. Pötschke, F. Guffarth, and D. Bimberg, *Phys. Rev. B* **71**, 155325 (2005).
- ¹⁰J. Persson, T. Aichele, V. Zwiller, L. Samuelson, and O. Benson, *Phys. Rev. B* **69**, 233314 (2004).
- ¹¹G. J. Beirne, M. Reischle, R. Roßbach, W. M. Schulz, M. Jetter, J. Seebeck, P. Gartner, C. Gies, F. Jahnke, and P. Michler, *Phys. Rev. B* **75**, 195302 (2007).
- ¹²R. Roßbach, M. Reischle, G. J. Beirne, M. Jetter, and P. Michler, *Appl. Phys. Lett.* **92**, 071105 (2008).
- ¹³W.-M. Schulz, R. Roßbach, M. Reischle, G. J. Beirne, M. Bommer, M. Jetter, and P. Michler, *Phys. Rev. B* **79**, 035329 (2009).
- ¹⁴M. Reischle, G. J. Beirne, W.-M. Schulz, M. Eichfelder, R. Roßbach, M. Jetter, and P. Michler, *Opt. Express* **16**, 12771 (2008).
- ¹⁵M. Reischle, G. J. Beirne, R. Roßbach, M. Jetter, and P. Michler, *Phys. Rev. Lett.* **101**, 146402 (2008).
- ¹⁶Y. Masumoto, K. Toshiyuki, T. Suzuki, and M. Ikezawa, *Phys. Rev. B* **77**, 115331 (2008).
- ¹⁷S. Kako, C. Santori, K. Hoshino, S. Götzinger, Y. Yamamoto, and Y. Arakawa, *Nature Mater.* **5**, 887 (2006).
- ¹⁸K. Sebald, P. Michler, T. Passow, D. Hommel, G. Bacher, and A. Forchel, *Appl. Phys. Lett.* **81**, 2920 (2002).
- ¹⁹A. Malko, D. Y. Oberli, M. H. Baier, E. Pelucchi, F. Michelini, K. F. Karlsson, M.-A. Dupertuis, and E. Kapon, *Phys. Rev. B* **72**, 195332 (2005).
- ²⁰B. Lounis, H. A. Bechtel, D. Gerion, P. Alivisatos, and W. E. Moerner, *Chem. Phys. Lett.* **329**, 399 (2000); S. Kimura, H. Kumano, M. Endo, I. Suemune, T. Yokoi, H. Sasakura, S. Adachi, S. Muto, H. Z. Song, S. Hirose, and T. Usuki, *Jpn. J. Appl. Phys.* **44**, L793 (2005).
- ²¹R. Brouri, A. Beveratos, J.-P. Poizat, and P. Grangier, *Opt. Lett.* **25**, 1294 (2000).
- ²²D. W. Snoke, J. Hübner, W. W. Rühle, and M. Zundel, *Phys. Rev. B* **70**, 115329 (2004).
- ²³E. Tsitsishvili, R. v. Baltz, and H. Kalt, *Phys. Rev. B* **67**, 205330 (2003).
- ²⁴J. Persson, M. Holm, C. Pryor, D. Hessman, W. Seifert, L. Samuelson, and M. E. Pistol, *Phys. Rev. B* **67**, 035320 (2003).
- ²⁵C. Pryor, M.-E. Pistol, and L. Samuelson, *Phys. Rev. B* **56**, 10404 (1997).
- ²⁶G. A. Narvaez, G. Bester, A. Franceschetti, and A. Zunger, *Phys. Rev. B* **74**, 205422 (2006).
- ²⁷M. Bayer, O. Stern, A. Kuther, and A. Forchel, *Phys. Rev. B* **61**, 7273 (2000).
- ²⁸J. Puls, M. Rabe, H.-J. Wünsche, and F. Henneberger, *Phys. Rev. B* **60**, R16303 (1999).